Theor Chem Acc (2007) 117:1085–1092
DOI 10.1007/s00214-006-0229-7

REGULAR ARTICLE

Molecular properties and stacking of 1-substituted hexaalkoxy triphenylenes

Luca Muccioli · Roberto Berardi · Silvia Orlandi · Matteo Ricci · Claudio Zannoni

Received: 2 August 2006 / Accepted: 13 October 2006 / Published online: 15 December 2006

Abstract In this work we consider the stability of columnar liquid crystals formed by discotic molecules differing only in one core substituent. In particular we concentrate on the 1-substituted 2, 3, 6, 7, 10, 11 hexaalkyloxy triphenylene family, and more specifically on the methoxy derivatives, studying the effects of seven α-substituents (H, Br, CH_3, Cl, F, NH_2, NO_2) on the shape and electronic properties, calculated at density functional level, and relating them with the phase behaviour of the corresponding hexyloxy derivatives. In a second step, we use the optimized structures and the atomic charges in a simplified Monte Carlo simulation of systems of molecules arranged in a columnar fashion, to try to shed light on the consequences of functionalization on the stacking behaviour.

Keywords Monte Carlo simulation · DFT · Discotics · Columnar phase · Electrostatic potential

1 Introduction

Since their discovery in 1977, discotic liquid crystals [1] have been the subject of intensive study because of their unique features resulting from the combination of self assembling, leading to columnar phases, and their interesting physical properties, such as negative birefringence, already exploited in optical compensating films [2]. Another feature of great interest of columnar systems is their strongly anisotropic (quasi-one-dimensional) charge transport [3], potentially useful in the realization of molecular wires and for other organic electronics applications [4]. Unfortunately, most of the desired physical properties cannot be obtained at the same time, and the final characteristics of a material often come from a delicate balance between competing effects [5]. Simulation techniques are potentially helpful for this required optimization task, but until now their application has been limited either to generic models [6] or to very small systems [7–9]. The difficult is due to the relatively large size of this class of molecules and to the fact that large samples of hundreds of molecules must be considered to obtain an equilibrium columnar phase by spontaneous self-assembly upon cooling from an isotropic phase. Thus, at the moment, the task of realistically simulating the various mesophases formed by discotics, including their self-assembly in columnar phases, is overambitious. On the other hand, the problem is often not that of understanding the formation of these columns but rather their stability and the changes of the columnar structure induced by even minor substitutions, and this is the task we would like to address here.

Among the discotic mesogenic core families, triphenylene is the most studied because of its richness of derivatives and applications [10,11]. The majority of triphenylene derivatives are symmetrically substituted with alkyl chains in the 2, 3, 6, 7, 10, 11 positions, but the functionalization of the less reactive 1- or α-position, initially performed to induce chirality in the mesophase, has emerged as a tool to modify the mesophase stability, probably in the hope of exploiting their dipolar interaction. In this sense, the stabilizing effect of electron-withdrawing substituents has already been recognized [12], while the extent of the distortion of the aromatic plane

L. Muccioli · R. Berardi · S. Orlandi · M. Ricci · C. Zannoni (✉)
Dipartimento di Chimica Fisica ed Inorganica and INSTM, Via Risorgimento, 4, 40136 Bologna, Italy
e-mail: Claudio.Zannoni@unibo.it

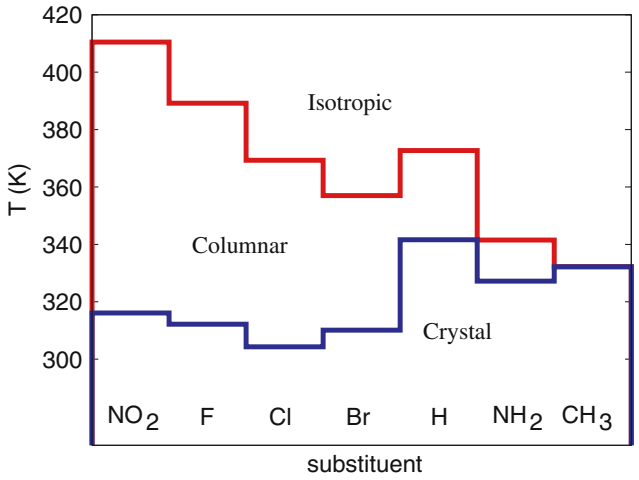

Fig. 1 Experimental transition temperatures for α-substituted hexahexyloxy triphenylenes; the compounds are ordered according to the temperature range ΔT_{col} of their columnar phase [12–14]

and of the conformational chirality and their effect on the columnar structure have still to be clarified.

In this paper we examine first the effect of seven different substituents in α-position (hydrogen, fluorine, chlorine, bromine, methyl, amino, nitro) on the molecular properties of hexamethoxy triphenylenes, and the relationship with the phase behaviour of the corresponding hexyloxy derivatives (Fig. 1); secondly, we study the properties of ideal stacks of the same compounds and we draw some indications on their stability.

2 Molecular properties

With the exception of some attempts in the past [12,13] with semiempirical methods, there is a lack of knowledge on the geometry and the charge distribution of triphenylenes; here we try to gain more insights through density functional methods [15], with the additional purpose of deriving some parameters required for the molecular simulations described in Sect. 3.

2.1 Computational details

In order to make the computation possible and to reduce the number of conformational degrees of freedom, we have limited the alkyl chains to a single methyl group. Even if we are not interested here on the effect of the length of the side chain, we find that at least one methyl group is needed to reproduce the intermolecular spacing along the column and to give a realistic twisting tendency. All the molecular geometries were optimised at quantum mechanical level with the following scheme: (1) geometry optimization with AM1 semiempirical method following the Hessian eigenvalues, in order to avoid local minima; (2) geometry optimization at B3LYP/3-21G level with gradient methods; (3) geometry optimization at B3LYP/6-31G level with gradient methods; (4) frequency calculation at B3LYP/6-31G level to test the correctness of the optimization; (5) final geometry optimization at B3LYP/6-311++G(d,p) level with gradient methods. Once obtained the molecular geometry, a single point B3LYP/6-311++G(d,p) calculation has been performed to calculate the electrostatic molecular properties, and an atomic point charge fit of the electrostatic potential and of the molecular dipole has been carried out, following the ESP scheme [16]. We have also calculated the dipole moments at the same level and the molecular polarizability at B3LYP/6-31G level.

2.2 Molecular shape

To quantify the distortion of the aromatic plane introduced by the substituent, we have determined the three bay dihedrals ω_i (Fig. 2, Table 1), which represent the angles between the pairs of interconnected aromatic rings. We find that the values range from $-10°$ to $+20°$ (taking the first angle as positive) and that the sum of three dihedrals never gives zero, thus indicating that the conjugation spreads out the distortion over the whole triphenylene plane and that phenyls are not perfectly coplanar. The value of ω_1 obtained for the nitro compound is in good agreement with the X-ray experimental value of 8.5° reported by Bushby et al. [17] for the crystal of the hexaethyl homologue, confirming that previously reported semiempirical calculations values overestimate the distortion effect [13] and are not quantitatively reliable for conjugated compounds, and in turn supporting

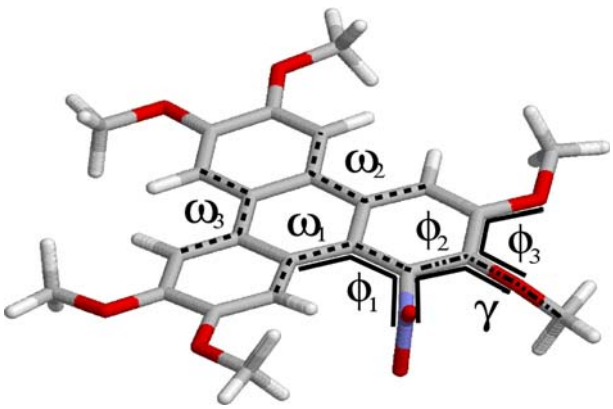

Fig. 2 Nitro-substituted triphenylene with the definition of plane distortion conformational angles ω_i (*single dashed lines*), ϕ_i (*continuos lines*) and γ (*double dashed line*)

Table 1 Ring distorsion angles ω_i, substituent angles ϕ_i and γ calculated at B3LYP/6-311++G(d,p) level (cfr Fig. 2)

Compound	ω_1	ω_2	ω_3	$\langle\|\omega_i\|\rangle$	ϕ_1	ϕ_2	ϕ_3	γ
HMOT	0.0	0.0	0.0	0.0	0.0	0.0	0.0	0.0
HMOT-Br	+19.8	+4.9	−9.9	11.5	+20.5	−4.2	−8.1	−103.1
HMOT-CH_3	+20.4	+4.7	−9.2	11.4	+16.4	−9.3	−2.1	+116.9
HMOT-Cl	+18.0	+3.7	−9.1	10.3	+16.6	−2.2	−7.5	−103.4
HMOT-F	+2.1	0.2	−0.8	1.0	+1.1	−4.3	3.4	+107.5
HMOT-NH_2	+17.8	+1.9	−7.7	9.1	+10.2	+1.8	−6.6	−110.8
HMOT-NO_2	+12.3	−2.0	−2.5	5.6	+5.4	−5.1	−0.2	+115.6

the choice of a higher level theoretical approach. We introduce as a convenient distortion index $\langle|\omega_i|\rangle$, the average of the absolute values of bay dihedrals, which can as well be considered a measure of the bulkiness of the substituents; in Table 1 we see that this index is remarkably low for fluorine and quite surprisingly for nitro (as this group has proven to lay with the two oxygens perpendicular to the molecular plane, hence limiting the steric repulsion), while it is around 10° for Cl, Br, NH_2 and CH_3 substituents. As the distortion of the aromatic rings is expected to limit the stacking capability of the molecules and consequentially to depress their columnar phase range, and as the nitro and the fluoro compounds present the highest mesophase stability and the lowest $\langle|\omega_i|\rangle$, this index is probably a good measure of the destabilization brought by a substituent to the columnar phase (cf Fig. 1).

The ring asymmetric distortion is indicative of conformational chirality, which is evidenced by the values of the bay angles ω_i, but also by the dihedrals ϕ_i in close proximity of the substituent (Fig. 2, Table 1); despite this, there are no experimental proofs of chiral columnar phases shown by this class of compounds. The functionalization in position 1 also has a strong influence on the conformation of the methoxy chain in position 2, with the O-methyl bond being forced by the steric repulsion to orient almost perpendicularly to the aromatic plane; this behaviour is evident from the values of the dihedral angle γ shown in Table 1. On the contrary, the conformation of the substituent in position 3 is only marginally influenced by the 1-substitution, which conserves the molecular core coplanarity, in disagreement with the output of semiempirical calculations [13].

2.3 Electrostatic potential

Moving now to the analysis of the electrostatic properties, we see from Table 2 that, as expected, the substitution determines the onset of a dipolar moment, whose magnitude depends on two factors: the difference in electronegativity between the substituent and the aromatic carbon, and the bulkiness of the substituent

Table 2 B3LYP/6-311++G(d,p) dipolar moments ($|\mu|$, Debye) and their components parallel and perpendicular to the molecular plane (μ_{ip},μ_{op}); B3LYP/6-31G diagonal static polarizabilities α_{iso} (au^3) and their components in (α_{ip}) and out (α_{op}) the molecular plane ($\alpha_{iso} = (2\alpha_{ip} + \alpha_{op})/3$)

Compound	μ_{ip}	μ_{op}	$\|\mu\|$	α_{ip}	α_{op}	α_{iso}
HMOT	0.00	0.00	0.00	411	116	312
HMOT-Br	2.81	2.04	3.47	426	130	328
HMOT-CH_3	1.88	0.56	1.96	419	135	324
HMOT-Cl	2.80	2.03	3.35	423	127	324
HMOT-F	3.13	1.13	3.33	411	118	313
HMOT-NH_2	1.12	0.43	1.20	418	126	320
HMOT-NO_2	5.79	0.53	5.81	422	138	328

that breaks the planar symmetry of the molecule. We have separated the dipole moments in two contributions: in–plane and out-of-plane (*ip* and *op* in Table 2): as a general trend, we find that the in-plane component is larger than the out-of-plane one. It is remarkable that compounds exhibiting a reduced or null tendency to columnar organization (i.e. NH_2 and CH_3 substituted) present smaller dipoles than the others. On the other hand, the top stable compounds (nitro and fluorine) exhibit the strongest in-plane dipole moment, suggesting that this plays an important role in columnar stability, while only the two bulkier substituents (Br, Cl) hold a strong out of plane dipole moment. We also report in Figs. 3, 4 the electrostatic potential maps (top and bottom views) drawn at the molecular van der Waals surface. We notice an almost indistinguishable pattern between halogenated compounds, especially for Cl and Br, which suggests us that substituent bulkiness is perhaps the major feature depressing columnar stability. On the other hand, apart from the substituent region and its close neighborhood, the overall qualitative shape of the charge distribution does not dramatically differ all over the considered compounds. The substitution also determines an increase of the overall molecular polarizability, also shown in Table 2, which as expected is larger in the molecular plane than out of plane. However, we cannot devise hints on columnar stability by looking at polarizabilities alone, which are in all cases very similar to each

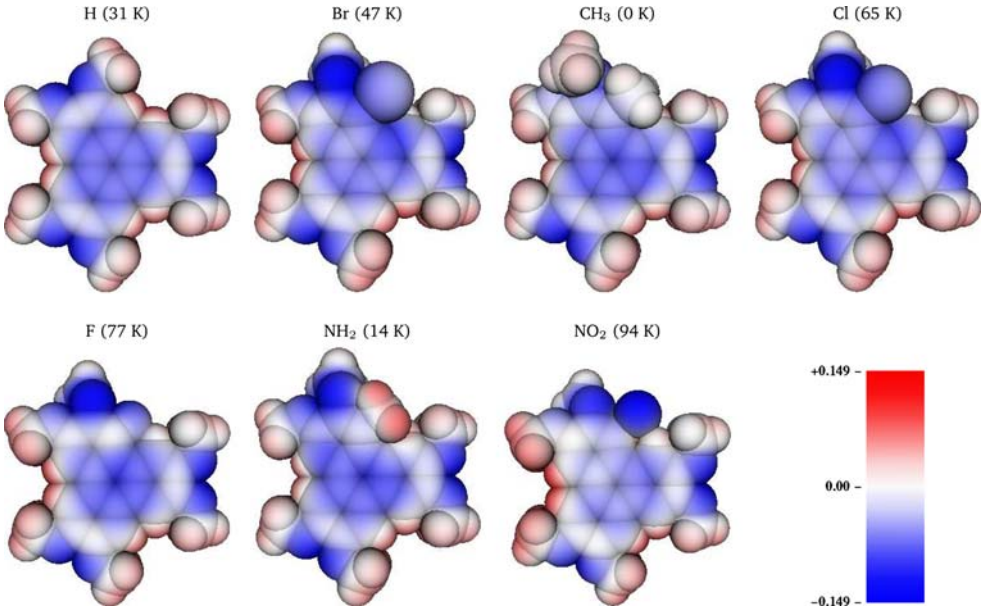

Fig. 3 Electrostatic potential maps (e/Å) at the molecular van der Waals surface of the compounds studied (*top view*; the *top side* is defined as the one towards the 1-substituent is bent). The columnar phase range is indicated in *parenthesis*

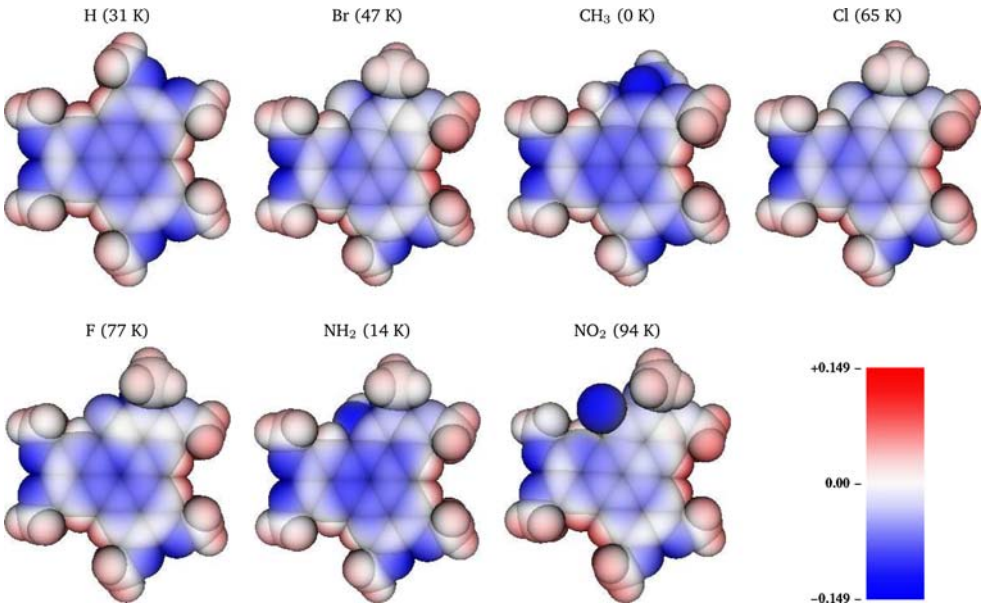

Fig. 4 Electrostatic potential maps (e/Å) at the molecular Van der Waals surface of the compounds studied (*bottom view*, see Fig. 3 for details)

other and essentially vary according to the volume of the substituent.

2.4 Transition temperatures and molecular features

As we mentioned in the introduction, determining transition temperatures from scratch via atomistic simulations is not yet feasible for discotics. However, it is interesting to try and relate the observed transitions to the molecular properties we have just determined. We observe first that the combination of the two contrasting effects of dipole and out-of-plane distortion seems sufficient in itself to qualitatively explain the trend in columnar temperature range, i.e. Br < Cl < F < H. More generally, it seems that an interplay between electrostatics and shape must be considered to interpret the columnar temperature range trend. To test the hypothesis that the columnar phase range is proportional to

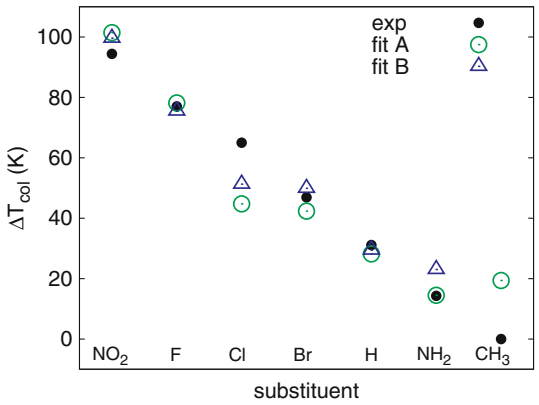

Fig. 5 Ranges of the columnar phase for each substituent: experimental (*filled circles, black*) [12–14], fitted using a linear dependence from dipole moments and $\langle|\omega_i|\rangle$ values (*empty circles, green,* fit A), fitted excluding the methyl substituted compound (*triangles, blue,* fit B)

electrostatic potential distortion, measured by the dipole moment, and inversely proportional to the distortion from planarity, we have attempted a least square fit of the phase ranges ΔT_{col} using the empiric equation $\Delta T_{\mathrm{col}} = T_0 + k_\mu \mu + k_\omega \langle|\omega_i|\rangle$ (Fig. 5), obtaining a standard deviation of 12.0 K when considering the methyl compound (fit A: $T_0 = 28.2$ K, $k_\mu = -3.6$ K/D, $k_\omega = 16.1$ K/deg) and a deviation of 7.8 K when excluding it (fit B: $T_0 = 29.4$ K, $k_\mu = -2.6$ K/D, $k_\omega = 14.6$ K/deg). In our opinion the agreement is satisfactory and the effects considered are sufficient to rationalize the columnar temperature range trend.

3 Stacking properties

3.1 Simulation settings

The molecular geometries and the point charges obtained by the DFT calculations have been used as input of a Monte Carlo simulation approach to evaluate the effects of geometry and charge distribution on single columns constituted by 50 molecules at the temperature of 350 K, employing periodic boundary conditions along the column direction in order to avoid boundary effects at its ends. The molecules have been assumed to be rigid, i.e. the structures have been kept fixed, while the intermolecular energy as been modelled as a sum of Lennard–Jones (OPLS [18]) and Coulomb contributions between DFT ESP fitting atomic charges. In a columnar phase molecules are partly kept in place by the action of the other surrounding columns; to somehow model this effect we have arbitrarily introduced an effective restoring potential by adding a harmonic spring with strength $k_R = 1$ kcal/(mol Å) that acts on the molecules whose center of mass lies at distance $r_{A,\perp} > r_R = 5$ Å from the column axis **Z**; this distance represents about the 40% of the diameter of the molecules under study. The energy expressions used are:

$$U_{\mathrm{tot}} = \sum_A \sum_B (U_{LJ}^{AB} + U_q^{AB}) + \sum_A U_R^A \tag{1}$$

$$U_{LJ} = 4 \sum_{i\in A} \sum_{j\in B} \sqrt{\epsilon_i \epsilon_j} \left[\left(\frac{\sigma_i + \sigma_j}{2 r_{ij}} \right)^{12} - \left(\frac{\sigma_i + \sigma_j}{2 r_{ij}} \right)^{6} \right] \tag{2}$$

$$U_q = \frac{1}{4\pi\epsilon_0} \sum_{i\in A} \sum_{j\in B} \frac{q_i\, q_j}{r_{ij}} \tag{3}$$

$$U_R = \sum_A \begin{cases} 0 & \text{if } r_{A,\perp} \le r_R \\ k_R (r_R - r_{A,\perp})^2 & \text{if } r_{A,\perp} > r_R \end{cases} \tag{4}$$

where A and B are two different molecules, i and j are two atoms of A and B at distance r_{ij}, σ_i and ϵ_i are Lennard–Jones parameters of the atom i, q_i is its atomic charge, ϵ_0 is the electric permittivity of free space, $\mathbf{r}_A$ is the position of molecule A and $\mathbf{r}_{A,\perp} = \mathbf{r}_A - \mathbf{Z}(\mathbf{Z} \cdot \mathbf{r}_A)$ is its projection perpendicular to the column axis. We have adopted a cutoff scheme based on molecules, i.e. the pair energy between molecule A and B is calculated only if they are at maximum five molecules apart from each other along the column; in practice this corresponds to a distance of about 18 Å. While the use of a cutoff for LJ potential is very common, the choice of a simple cutoff method for the electrostatic potential is justified by the fact that the interaction energy between two neutral molecules decreases monotonically with the intermolecular distance [19,20], and by the fact that we are dealing with a single isolated column.

The Monte Carlo evolution of molecular positions and orientations was achieved performing alternatively rotational, translational, rototranslational moves and random scaling of the overall column length. The existence of two conformational isomers (with barriers ≈ 1–10 kcal/mol [12]) and two possible orientations of the out-of-plane component of the molecular dipole may in turn stabilize a chiral or an antiferroelectric arrangement in the column; to not rule out the formation of these types of columns, we have also attempted moves that invert the molecular chirality (through a mirror reflection with respect to the molecular plane) and moves that invert the out-of-plane molecular dipole (through a rotation of 180° about the molecular x axis of inertia). For all compounds, the starting configuration was a perfect column with all the molecules laying parallel with the same orientation at the intermolecular distance of 6 Å. The columns were equilibrated for

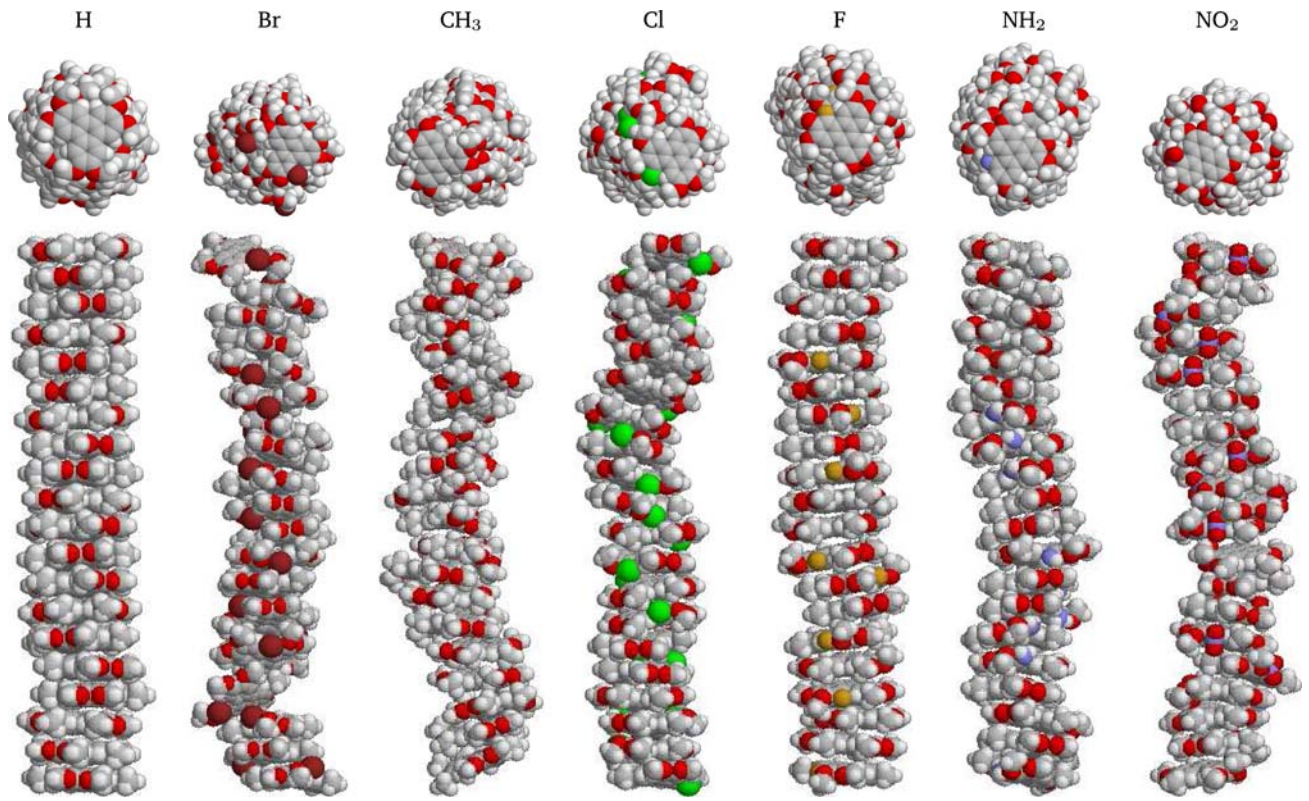

Fig. 6 Snapshots of a 20-molecules segment of the simulated columns (*top* and *side views*)

about 10^6 cycles, followed by production runs of the same length.

3.2 Simulation results

To start the analysis of the simulation outcomes, a glance to the column portions reproduced in Fig. 6 can give a qualitative impression of the effects of substitution: with the exception of fluorine, the stacking becomes more irregular, with an increasing tendency of molecules to tilt and to move laterally with respect to the column center, and the onset of possible defects especially for bulkier substituents such as bromine and methyl.

An inspection of the average energies (reported in Table 3) reveals that the stacking is dominated by the Lennard–Jones (i.e. dispersive) interactions and that the strongest intermolecular interaction is registered for the unsubstituted compound. This finding is not easy to relate to the greater columnar stability of most of the substituted compounds, and might be due either to the fixed geometry approximation, which of course affects in greater extent the substituted compounds, or to a destabilization of the attendant crystal phase. The comparison of the various contributions with respect to the HMOT-H values underlines the stabilizing effect of the electrostatic energy induced by the substituent, which is maximum for NO_2, and the decrease of the Lennard–Jones energy, proportional to the encumbrance of the moiety in position 1. Looking to the effects on the column geometry, it is apparent from the average of $r_\perp$ and $r_\parallel$ in Table 3 that substitution depresses the regularity and the stacking capability of the molecules, which are forced by steric interaction to reduce the cofaciality and to increase the intermolecular distance. The values of $r_\parallel$ for the H- and nitro-substituted can be compared with the experimental data available: 3.46 Å for hexabuthyloxy derivative in the columnar phase [17] and 3.54 Å of nitro-hexaethyloxy derivative in the crystal phase

Table 3 Average column properties calculated from simulation: total ($\langle U_{\text{tot}} \rangle$), Lennard-Jones ($\langle U_{LJ} \rangle$), electrostatic ($\langle U_q \rangle$) and restoring ($\langle U_R \rangle$) energies per molecule (kcal/mol), lateral displacement $\langle r_\perp \rangle$ and intermolecular distance projected along the column axis, $\langle r_\parallel \rangle$ (Å)

Column	$\langle U_{\text{tot}} \rangle$	$\langle U_{LJ} \rangle$	$\langle U_q \rangle$	$\langle U_R \rangle$	$\langle r_\perp \rangle$	$\langle r_\parallel \rangle$
HMOT-Br	−21.1	−21.4	0.3	0.06	2.97	3.88
HMOT-CH_3	−22.0	−22.2	0.2	0.01	2.55	3.89
HMOT-Cl	−23.8	−24.7	0.9	0.00	2.55	3.72
HMOT-F	−26.6	−26.7	0.1	0.00	2.43	3.54
HMOT-NH_2	−24.3	−25.0	0.6	0.00	2.49	3.73
HMOT-NO_2	−24.3	−23.4	−1.0	0.02	2.75	3.75
HMOT-H	−27.4	−28.7	1.3	0.00	0.86	3.46

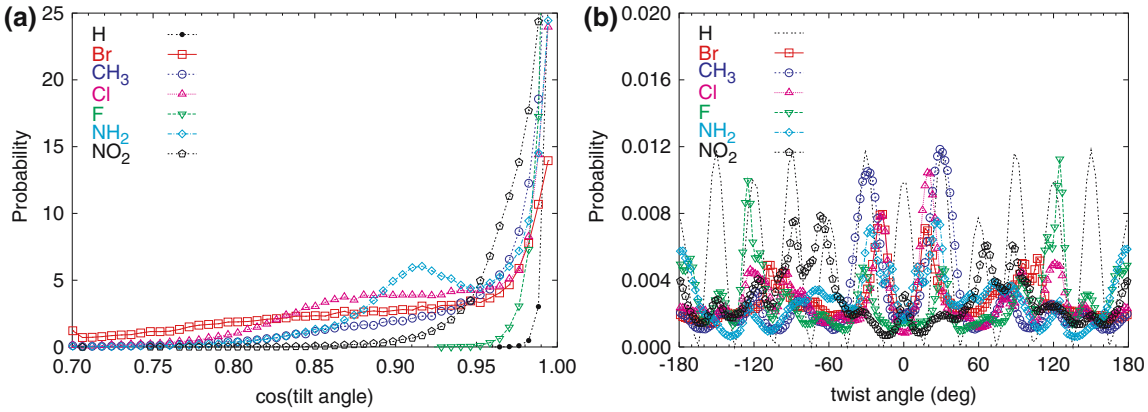

Fig. 7 Distribution of the tilt angle between the molecular plane and the column axis (**a**) and of the twist angle between to neighbouring molecular plane and the column axis (**b**)

[21]. The comparison with the simulation of HMOT-H is surprisingly good, while this distance appears to be slightly overestimated for the nitro compound. Another important factor for the design of good molecular wires is the possibility of tuning the angle between the molecular plane and the column axis (tilt), and the variation of angle of rotation about the molecular axis between to adjacent molecules (twist); in particular the latter have been shown to be fundamental for controlling the orbital overlap and the related charge transport capability [5]. Here we see that the 1-functionalization of the triphenylene core determines a broadening of the tilt angle distribution (Fig. 7a) and more interestingly the asymmetrization of the twist angle distribution (Fig. 7b), hinting at the possibility of selecting a specific substituent with the aim of obtaining a determined value of the twist angle.

4 Conclusions

This density functional study on hexaalkyloxy triphenylenes indicates that introducing an electrowithdrawing function in position 1 is an effective way of stabilizing the columnar phase only if the molecular planarity can be retained. On this basis, we have derived an empirical equation to calculate the columnar phase range of a given substituent from the calculated dipole moments, which is a measure of the electro-withdrawing strength, and the average bay dihedrals $< |\omega_i| >$, which account for the distortion from planarity.

The Monte Carlo simulations, performed on ideal columns with the DFT molecular geometries, indicate that the 1-substitution increases the positional and orientational disorder of the stack, and noticeably desymmetrizes the twist angle distribution. This effect could be possibly exploited to maximize the orbital overlap between the column neighbours in order to improve one-dimensional conductivity. This type of functionalization instead does not seem instead a good strategy to achieve an overall column chirality or ferroelectricity.

The column simulating scheme derived here, possibly combined with semiempirical calculations of mobility along the column [22] could be employed as a systematic tool for comparing and selecting different cores in view of optimizing the charge transport prior to eventually proceed to the actual synthesis.

Acknowledgements We gratefully acknowledge the Italian Ministery of University and Reseach and the European Union for supporting this study through the project PRIN "Modelling and characterisation of liquid crystals for nano-organised structures" and the EU Integrated Project NAIMO (No NMP4-CT-2004-500355).

References

1. Demus D, Goodby J, Gray GW, Spiess HW, Vill V (eds) (1998) Handbook of liquid crystals. Wiley-VCH, New York
2. Mori H, Itoh Y, Nishiura Y, Nakamura T, Shinagawa Y (1997) Jpn J Appl Phys 36:143
3. Adam D, Schumacher P, Simmerer J, Haussling L, Siemensmeyer K, Etzbach KH, Ringsdorf H, Haarer D (1994) Nature 371:141
4. Boden N, Movaghar B (1998) Handbook of liquid crystals, vol 2B, chap IX. Wiley-VCH, New York
5. Lemaur V, da Silva Filho DA, Coropceanu V, Lehmann M, Geerts Y, Piris J, Debije MG, van de Craats AM, Senthilkumar K, Siebbeles LDA, Warman JM, Brédas JL, Cornil J (2004) J Am Chem Soc 126:3271
6. Berardi R, Cecchini M, Zannoni C (2003) J Chem Phys 119:9933
7. Cinacchi G, Colle R, Tani A (2004) J Phys Chem B 108:7969
8. Maliniak A (1992) J Chem Phys 96:2306
9. Mulder FM, Stride J, Picken SJ, Kouwer PHJ, de Haas MP, Siebbeles LDA, Kearley G (2003) J Am Chem Soc 125:3860

10. Cammidge AN, Bushby RJ (1998) Handbook of liquid crystals, vol 2B, chap VII. Wiley-VCH, New York
11. Kumar S (2004) Liq Cryst 31:1037
12. Praefcke K, Eckert A, Blunk D (1997) Liq Cryst 22:113
13. Boden N, Bushby R, Cammidge A, Duckworth S, Headdock G (1997) J Mat Chem 7:601
14. Boden N, Bushby RJ, Cammidge AN, Headdock G (1995) Synthesis:31
15. Cramer CJ (2002) Essentials of computational chemistry. Wiley, New York
16. Besler BH, Merz KM Jr, Kollman PA (1990) J Comput Chem 11:431
17. Bushby RJ, Boden N, Kilner CA, Lozman OR, Lu Z, Liu Q, Thornton-Pett MA (2003) J Mat Chem 13:470
18. Jorgensen WL, Maxwell DS, Tirado-Rives J (1996) J Am Chem Soc 118:11, 225–11, 236
19. Berardi R, Muccioli L, Orlandi S, Ricci M, Zannoni C (2004) Chem Phys Lett 389:373
20. Wolf D, Keblinski P, Phillpot SR, Eggebrecht J (1999) J Phys Chem 110:8254
21. Destrade C, Mondon MC, Malthête J (1979) J Phys Colloq 40C3:17
22. Olivier Y, Lemaur V, Brédas JL, Cornil J (2006) J Phys Chem A 110:6356